Thermochimica Acta 497 (2010) 124–128

Contents lists available at ScienceDirect

Thermochimica Acta

journal homepage: www.elsevier.com/locate/tca

Thermodynamic studies of mixtures for topical anesthesia: Lidocaine–salol binary phase diagram

Mathieu Lazerges, Ivo B. Rietveld*, Yohann Corvis, René Céolin, Philippe Espeau

Laboratoire de Chimie Physique (EA 4066), Faculté des Sciences Pharmaceutiques et Biologiques, Université Paris Descartes, 4 Avenue de l'Observatoire, 75270 Paris Cedex 06, France

ARTICLE INFO

Article history:
Received 20 July 2009
Received in revised form 24 August 2009
Accepted 26 August 2009
Available online 2 September 2009

Keywords:
Topical anesthesia
Eutectic mixtures
Lidocaine
Salol
Phase diagram
EMLA

ABSTRACT

The lidocaine–salol binary system has been investigated by differential scanning calorimetry, direct visual observations, and X-ray powder diffraction, resulting in a temperature-composition phase diagram with a eutectic equilibrium. The eutectic mixture, found at 0.423 ± 0.007 lidocaine mole-fraction, melts at $18.2 \pm 0.5\,^{\circ}C$ with an enthalpy of $17.3 \pm 0.5\,kJ\,mol^{-1}$. This indicates that the liquid phase around the eutectic composition is stable at room temperature. Moreover, the undercooled liquid mixture does not easily crystallize. The present binary mixture exhibits eutectic behavior similar to the prilocaine–lidocaine mixture in the widely used EMLA® topical anesthetic preparation.

1. Introduction

The first successful mixture of pharmaceutical compounds for topical anesthesia is most likely Bonain's mixture. In 1898, Jules-Aristide Bonain (1860–1934), a former surgeon of the French Navy, discovered that mixtures of cocaine hydrochloride, phenol, and menthol spontaneously transform into homogeneous liquids at room temperature [1]. The mixture in fractions of equal weight is still called Bonain's mixture. Bonain explained liquefaction by interactions leading to a 'menthyl-phenate' acting as a solvent for cocaine hydrochloride [2]. In the light of classical thermodynamics, this phenomenon is nowadays related to the formation of a eutectic equilibrium.

Due to the side effects of cocaine and caustic properties of phenol, Bonain's mixture is nowadays rather seldom used. Instead, a 'eutectic mixture of local anesthetics' (EMLA), an emulsion containing equal masses of lidocaine and prilocaine, was developed in 1980 by Astra (Sweden) for use in creams [3,4]. It is still the more widely employed, although pharmacologically inactive compounds have been suggested instead of prilocaine, after it was published that the latter may provoke methaemoglobinemia [5,6]. Other eutectic mixtures based on lidocaine were subsequently patented [7]; thymol, menthol, methyl salicylate, salol (phenyl salicylate), butylated hydroxytoluene, butylated hydroxyanisole, S(+)-ibuprofen, R(−)-ibuprofen, cineole, eugenol, capsaicin and eucalyptol were claimed as pharmaceutically inactive components for eutectic mixtures with lidocaine. Surprisingly, only two studies on these combinations have been published so far. The study on lidocaine–menthol reports a eutectic point at 26 °C and 0.30 lidocaine weight fraction [8]. The study on lidocaine–thymol reports a liquid range at 25 °C from 0.30 to 0.70 lidocaine weight fraction, without information about the eutectic point [9]. To our knowledge, no experimental data on the other binary systems have been published, despite their potential to form eutectic systems suitable for topical anesthesia.

To start with, eutectic points for various compounds from patent [7] can be calculated assuming ideal liquid behavior (Fig. 1). The position of these ideal eutectic points should help finding compounds that are likely to form eutectic equilibria with lidocaine below room temperature. It can be seen that besides prilocaine and L-menthol, salol appears to be a good candidate, which, in addition, exhibits a very low toxicity [15].

A study of the salol–lidocaine (Fig. 2) binary system is reported in this paper as part of a more general investigation into eutectic binary systems based on lidocaine. Some properties from literature are compiled in Table 1. Literature does not report if the metastable form of salol, melting at 30 °C, is identical to the metastable monoclinic crystal structure.

2. Materials and methods

2.1. Chemicals

Lidocaine ($C_{14}H_{22}N_2O$, $M = 234.34\,g\,mol^{-1}$) of medicinal grade was obtained from former Roger Bellon Lab. (now Sanofi Aventis).

* Corresponding author. Tel.: +33 1 53739675; fax: +33 1 53739676.
E-mail address: ivo.rietveld@parisdescartes.fr (I.B. Rietveld).

0040-6031/$ – see front matter © 2009 Elsevier B.V. All rights reserved.
doi:10.1016/j.tca.2009.08.016

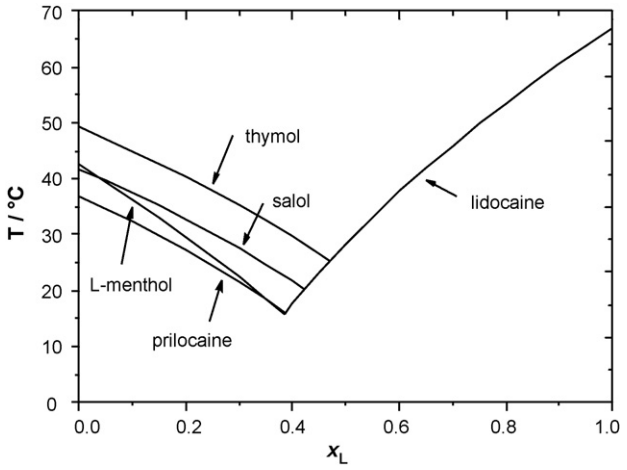

Fig. 1. Temperature–lidocaine mole fraction (T–x_L) diagram showing the ideal liquidus curves of a number of compounds (left) mentioned in patent [7] and of lidocaine (right). The points of intersection are the eutectic points in case of ideal liquid behavior. Liquidus curves were calculated with melting point and heat of fusion data from literature (lidocaine [10], L-menthol [11], prilocaine [4], salol [12] and thymol [13,14]).

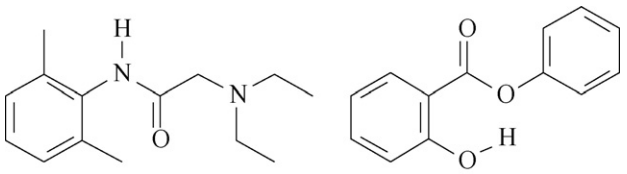

Fig. 2. Structure of lidocaine (left) and salol (right).

Salol ($C_{13}H_{10}O_3$, $M = 214.22\,g\,mol^{-1}$) was purchased from ACROS ORGANICS (France) (purity ≥ 99%). Both compounds were used as obtained.

2.2. Differential scanning calorimetry (DSC)

Differential scanning calorimetry experiments were performed using two Mettler-Toledo (Switzerland) 822e thermal analyzer's equipped with a Huber (Germany) TC100 cooling device for measurements down to −80 °C. Indium ($T_{fus} = 156.60\,°C$, $\Delta_{fus}H = 3267\,J\,mol^{-1}$) and zinc ($T_{fus} = 419.53\,°C$, $\Delta_{fus}H = 7320\,J\,mol^{-1}$) were used for calibration of temperature and enthalpy. Specimens were weighed with a microbalance sensitive to 0.01 mg and sealed in aluminum pans. DSC runs were performed at $5\,K\,min^{-1}$.

Preliminary DSC measurements indicated that crystallization from the homogeneous melt was rarely observed on cooling to −50 °C; therefore, two different approaches were employed to obtain solid mixtures at thermodynamic equilibrium. One approach was by temperature cycling. Components in various ratios were molten to form homogeneous liquids and then cooled down to −50 °C. Multiple heating and cooling cycles (between −50 °C and 10 °C) were necessary to fully crystallize the mixtures. The other approach to prepare solid mixtures was by mechanically grinding lidocaine and salol with pestle and mortar at temperatures between −5 °C and 5 °C, well below the eutectic temperature.

Table 1
Lidocaine and salol literature data.

	Melting temperature (°C)	Melting enthalpy ($kJ\,mol^{-1}$)	References
Lidocaine			
Monoclinic			Hanson and Banner [17] and Bambagiotti-Alberti et al. [16]
	67	15.30	Chickos and Nichols [10]
	67.0 ± 0.5		Cui and Frank [18]
Salol (phenyl salicylate)			
Rhombohedral			Flachsbart [19]
	40.6		Levi [20]
	41.70		Timmermans and Burriel [21]
	41.81 ± 0.01	19.16 ± 0.02	Hanaya et al. [12]
	41	18.6 ± 0.2	Moura Ramos et al. [22]
Metastable phase			
	30.4		Lesnik and Danilov [23]
	30	16.5	Moura Ramos et al. [22]
Monoclinic[a]			Hammond et al. [24]

[a] The melting point of the metastable monoclinic phase was not reported.

2.3. Visual observation of the liquidus

Accurate determination of the liquidus temperature near the eutectic composition is difficult with DSC, because the liquidus-related thermal effect is small and partially merges with the much larger thermal effect of the eutectic transition. Therefore, liquidus compositions have been determined by direct visual observation at room temperature. Small amounts of solid lidocaine of known mass were added from time to time to a liquid mixture starting from the eutectic composition until dissolution was no longer observed. This allowed the lidocaine-rich liquidus to be determined within two compositions. The procedure was repeated with salol in order to obtain the composition of the salol-rich liquidus. The observations were repeated several times at room temperature and the average temperature and compositions were determined.

2.4. High-resolution X-ray powder diffraction (XRPD)

X-ray powder diffraction patterns were recorded using a CPS120 position sensitive detector from INEL (France) and Kα1 radiation (1.7889 Å) from a cobalt anode. The specimens were introduced in capillary tubes (0.5 mm diameter) made of Lindemann glass from Hilgenberg (Germany).

3. Results and discussion

3.1. Pure components

3.1.1. Lidocaine

Lidocaine literature data are given in Table 1. The monoclinic crystal structure of lidocaine used in this study was confirmed by high-resolution X-ray powder diffraction. DSC experiments at various heating rates on two analyzers (26 runs) showed that lidocaine melts at 67.5 ± 0.4 °C with an enthalpy of 16.4 ± 0.2 $kJ\,mol^{-1}$ (69.8 ± 0.7 $J\,g^{-1}$) and that the melt crystallizes on cooling between 15 °C and 27 °C. The enthalpy of fusion is found to be 7% higher than reported in literature (Table 1) [10,18].

3.1.2. Salol

Salol literature data are given in Table 1. The rhombohedral structure of salol used in the present study was confirmed by high-resolution X-ray powder diffraction. DSC experiments at various heating rates on two analyzers (39 runs) resulted in a melting point for rhombohedral salol of 41.9 ± 0.5 °C with a melting enthalpy of 19.2 ± 0.5 $kJ\,mol^{-1}$ (90 ± 3 $J\,g^{-1}$). Salol recrystallizes between −18 °C and −12 °C.

A metastable phase was obtained by quenching undercooled liquid at room temperature in liquid nitrogen (−196 °C) [22]. DSC experiments at various heating rates on two analyzers (5 runs) resulted in a melting point for this metastable phase at 30.8 ± 0.3 °C,

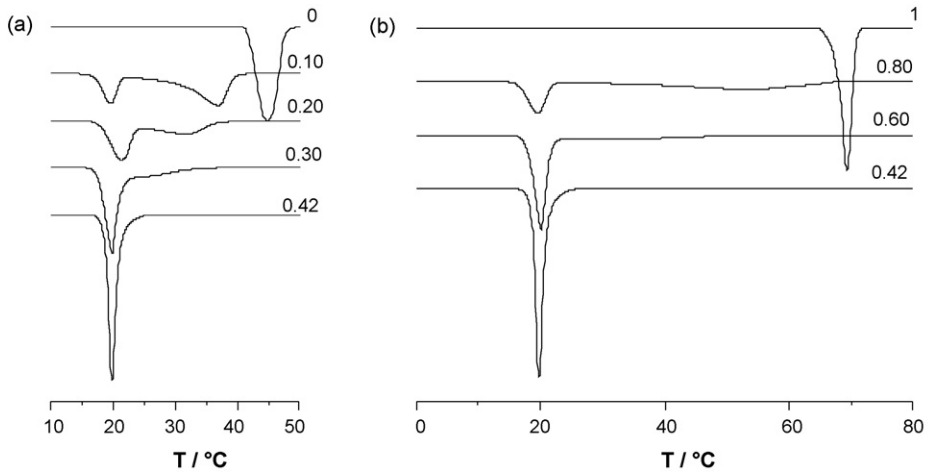

Fig. 3. DSC-curves (5 K min^{-1}) of salol–lidocaine mixtures for lidocaine mole fractions of: (a) 0 (pure salol) to 0.42 (close to eutectic composition) and (b) 1 (pure lidocaine) to 0.42.

with a melting enthalpy of 17.7 ± 0.2 kJ mol^{-1} (83 ± 1 J g^{-1}), and a crystallization range between -14 °C and 0 °C.

3.2. Lidocaine–salol temperature-composition phase diagram

From the DSC experiments, it appeared that liquid mixtures of salol and lidocaine only fully crystallize in a limited region on the salol-rich side of the phase diagram ($0 < x_L < 0.36$, x_L = lidocaine mole fraction) and even in this region, equilibrium is not easily reached as can be judged from the large number of temperature cycles before the stable phases crystallize. Complete crystallization of liquid mixtures was not observed on the lidocaine-rich side; in fact, a crystallization peak was observed (not shown), related to the crystallization of lidocaine in excess, confirmed by an increase of its size relative to the lidocaine content in the mixture.

As described in Section 2, the two solids were also mechanically mixed well below the eutectic temperature. Typical DSC-curves for both sample preparation methods are shown in Fig. 3a for the salol-rich side and Fig. 3b for the lidocaine-rich side. One can observe the evolution of the liquidus temperature and enthalpies of transition from the pure compounds to the eutectic point.

Visual observation of the liquidus gave rise to two liquidus points on either side of the eutectic composition: lidocaine-sided liquidus at $x_L = 0.436 \pm 0.005$ and 23.5 ± 1 °C and salol-sided liquidus at $x_L = 0.372 \pm 0.005$ and 23.7 ± 1 °C.

The salol-lidocaine phase diagram is presented in Fig. 4a. The Tammann plot shows that the eutectic composition is $x_L = 0.43 \pm 0.01$ and that the shift of the eutectic equilibrium for this composition was accompanied by an enthalpy change of 17.3 ± 0.5 kJ mol^{-1} (Fig. 4b). The temperature corresponding to the eutectic equilibrium obtained from the DSC experiments (Fig. 3) is 18.2 ± 0.5 °C.

The liquidus curves do not follow ideal behavior. In particular, the lidocaine-rich liquidus points are found underneath the ideal curve. For the salol-rich side, the scatter of the obtained liquidus points is larger, but most points are found above the ideal curve. The liquidus points over the entire range of compositions have been fitted simultaneously taking into account excess Gibbs energy of mixing with a Redlich–Kister polynomial and assuming complete immiscibility in the solid phase, according to a previously described procedure [25–27]. The resulting liquidus curves are shown in Fig. 4a. The lidocaine-rich liquidus curve is lower than the ideal curve, indicating that lidocaine liquefies more readily in the presence of salol. On the salol-rich side of the phase diagram, the liquidus is higher than the ideal curve indicating that salol somewhat resists the solid to liquid transition in the presence of lidocaine. The fitted liquidus intersects the ideal liquidus at about $x_L = 0.36$, marking the point where the liquid becomes stabler than in the ideal case. The increased liquid stability for mixtures from

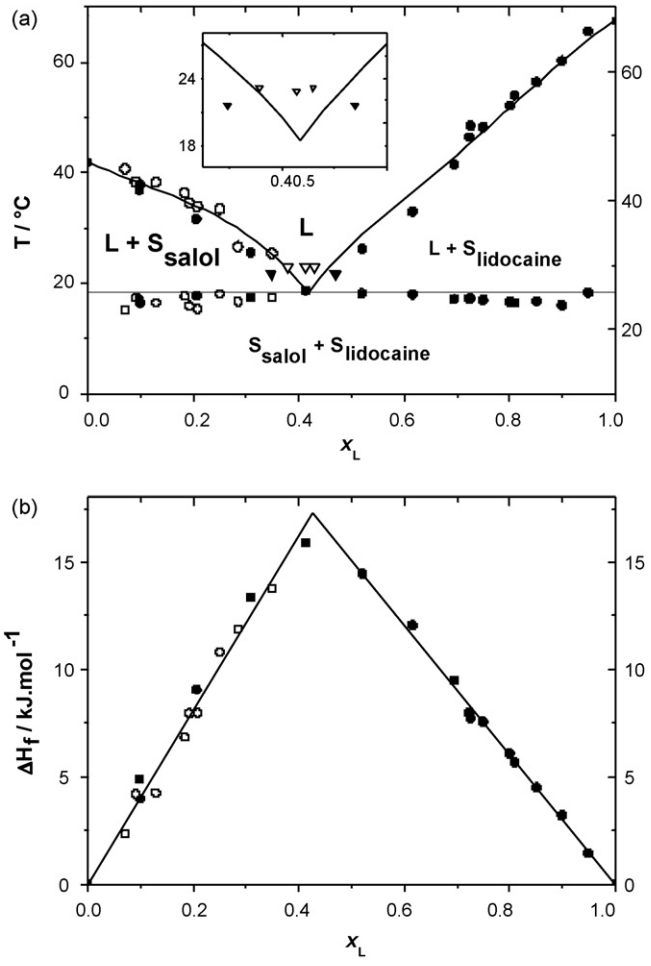

Fig. 4. Salol–lidocaine phase diagram (a) and Tammann plot related to the eutectic equilibrium line (b). Filled circles correspond to samples mechanically mixed between -5 °C and 5 °C (DSC measurements), open circles are obtained by recrystallization from a homogeneous liquid mixture (DSC measurements), inverted triangles are obtained by direct visual observation of binary mixtures (inset): open triangles indicate homogeneous liquid, filled triangles indicate mixture of liquid and solid.

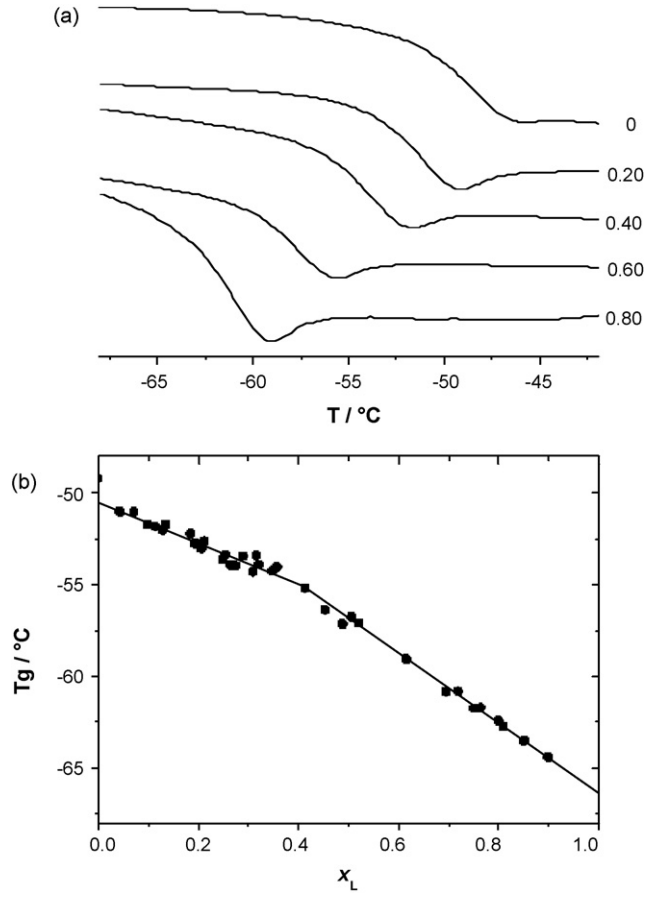

Fig. 5. (a) DSC-curves of undercooled lidocaine–salol liquid mixtures for $x_L = 0$ (pure salol) to 0.8. Samples at 75 °C (melt), were quenched at −196 °C then immediately heated at a 5 K min^{-1} rate from −80 °C. (b) Midpoint glass transition temperature versus x_L.

$x_L \geq 0.36$ is supported by the observation that solutions from about $x_L = 0.36$, once molten, do not recrystallize but remain undercooled liquids below the eutectic temperature (Fig. 4a). The fit gives rise to a eutectic point at the intersection of the two calculated liquidus curves: $x_L = 0.418$ and $T = 18.4$ °C. The eutectic temperature is identical (within error) to the value found by DSC measurement. The eutectic composition, averaged with the result from the Tammann plot, is therefore $x_L = 0.423 \pm 0.007$.

The formation of solid solutions at the sides of the binary phase diagram in either lidocaine-rich ($x_L = 0.946$) or salol-rich ($x_L = 0.900$) mixtures has been excluded by X-ray diffraction experiments. For both, no change in the positions of the Bragg peaks was observed with respect to the pattern of each pure component. In addition, both lines in the Tammann plot extrapolate neatly to $x_L = 0$ and 1, which also confirms the absence of solid solutions on either side of the phase diagram. These results justify the assumption of complete immiscibility in the solid phase used for the phase diagram calculations.

3.3. Glass transition in the undercooled binary mixtures

Binary liquid mixtures held at a temperature of 75 °C were quenched at −196 °C by immersion in liquid nitrogen. The resulting samples were studied by DSC from −80 °C to −40 °C at 5 K min^{-1}; the DSC-curves are shown in Fig. 5a. A glass transition is found for pure salol and all the mixtures, except for pure lidocaine, thus indicating that all quenched mixtures formed glasses. Whereas mixtures rich in salol crystallize after repeated temperature cycling, liquid of the eutectic composition seemed remarkably stable and never crystallized during the experiments. In the lidocaine-rich mixtures, the part representing the eutectic composition never crystallized, but surplus lidocaine did, which was concluded from an exothermic peak equal to the crystallization enthalpy of lidocaine in excess.

The glass transition temperature decreases with increasing lidocaine concentration. This evolution can be divided in two parts abruptly changing at $x_L = 0.41$, each being virtually linear with lidocaine composition (Fig. 5b). Why there is a change in the decrease of the glass transition temperature and if there is a relation with the eutectic composition remains a matter of study.

Table 2
Homogeneous liquid range in mole fraction lidocaine (x_L) for four of its binary mixtures at room temperature (25 °C), measured and ideal liquid behavior.

Second component	Measured composition x_L	Ideal composition x_L
Prilocaine	0.37–0.54	0.25–0.46
L-menthol	0.22[a] (26 °C)	0.27–0.46
Thymol	0.22–0.60	0.47[a] (25.5 °C)
Salol	0.35–0.48	0.35–0.46

[a] A single value implies that the eutectic temperature is located above room temperature. In those cases, the eutectic composition has been given with its temperature between parentheses.

4. Concluding remarks

The binary temperature–composition (T–x) phase diagram of salol and lidocaine consistent with stable phase behavior has been obtained. From the homogeneous liquid, stable solid mixtures are not easily obtained; the undercooled liquid is relatively stable, especially on the lidocaine-rich side. A shift of the lidocaine-sided liquidus to lower temperatures in comparison to ideal liquid behavior confirms an increased stability for the liquid phase at these compositions. Mechanically prepared solid mixtures provided the same eutectic temperature and the same liquidus temperatures as solid mixtures obtained from the homogeneous liquid. The former were used to obtain the phase transition data for the compositions where the homogeneous liquid failed to recrystallize.

The eutectic composition is found to be $x_L = 0.423 \pm 0.007$ at a temperature of 18.2 ± 0.5 °C. Its enthalpy of transition is 17.3 ± 0.5 kJ mol^{-1}. X-ray measurements and the Tammann plot point to the absence of limited solid solutions at either side of the phase diagram.

The undercooled liquid phase exhibits a glass transition. The midpoint temperature decreases linearly with increasing lidocaine mole fraction; however, near the eutectic composition, an abrupt change in the slope is observed.

To compare the three published lidocaine-based binary systems and the system salol–lidocaine, the minimum and maximum compositions of the liquid phase regions at room temperature have been compiled in Table 2. The binary mixture with prilocaine has a liquid range shifted towards lidocaine. Prilocaine dissolved in lidocaine liquefies more readily than in the ideal case, whereas lidocaine dissolved in prilocaine destabilizes the homogeneous liquid to a larger extent than in the salol–lidocaine system. For lidocaine binary mixtures with L-menthol or thymol, either the predicted liquid range is replaced by a eutectic point shifted to the lidocaine-poor side or the predicted eutectic point is replaced by a wide liquid range respectively. In the case of thymol–lidocaine, it would be interesting to investigate if the liquid mixture rich in lidocaine is in fact an undercooled liquid, because lidocaine-rich solutions seem prone to such behavior (cf. salol–lidocaine).

If the lidocaine content in anesthetic creams should be as high as possible, the prilocaine binary mixture seems, at present, still the most effective and most stable. If the side effects of prilocaine cause

a problem, it can be replaced by salol. In that case, the maximum concentration of lidocaine in the binary mixture will be reduced with 0.06 (mole fraction).

References

[1] A. Bonain, Bulletins et mémoires de la société Française d'otologie, de Laryngologie 14 (1899) 559–563.
[2] J. Tainmont, B-ENT 3 (2007) 217–230.
[3] B.F.J. Broberg, H.C.A. Evers, Local anesthetic mixture for topical application, and process for its preparation, as well as method for obtaining local anesthesia EP0002425 (A1) (1981).
[4] A. Brodin, A. Nyqvist-Mayer, T. Wadsten, B. Forlsund, F. Broberg, J. Pharm. Sci. 73 (1984) 481–484.
[5] M. Tryba, H. Kurth, M. Zenz, Reg. Anaesth. 10 (1987) 31–36.
[6] F.G. Vasters, L.H.J. Eberhart, T. Koch, P. Kranke, H. Wulf, A.M. Morin, Eur. J. Anaesth. 23 (2006) 760–765.
[7] H.W. Jun, L. Kang, Enhanced transdermal anesthesia of local anesthetic agents, WO0069471 (A1) (1999).
[8] L. Kang, H.W. Jun, J.W. McCall, Int. J. Pharm. 206 (2000) 35–42.
[9] L. Kang, H.W. Jun, N. Mani, Int. J. Pharm. 222 (2001) 35–44.
[10] J.S. Chickos, G. Nichols, J. Chem. Inf. Comput. Sci. 42 (2002) 368–374.
[11] H. Yuasa, M. Ooi, Y. Takashima, Y. Kanaya, Int. J. Pharm. 203 (2000) 203–210.
[12] M. Hanaya, T. Hikima, M. Hatase, M. Oguni, J. Chem. Thermodyn. 34 (2002) 1173–1193.
[13] D.R. Lide (Ed.), CRC Handbook of Chemistry and Physics, 77th ed., CRC Press, Boca Raton, 1996.
[14] C.H. Sorum, E.A. Durand, J. Am. Chem. Soc. 74 (1952) 1071–1073.
[15] A. Lapczynski, L. Jones, D. McGinty, S.P. Bhatia, C.S. Letizia, A.M. Api, Food Chem. Toxicol. 45 (2007) S472–476.
[16] M. Bambagiotti-Alberti, B. Bruni, M. Di Vaira, V. Giannellinia, A. Guerric, Acta Crystallogr. E 63 (2007) 768–779.
[17] A.W. Hanson, D.W. Banner, Acta Crystallogr. B: Struct. Sci. 30 (1974) 2486–2488.
[18] Y. Cui, S.G. Frank, J. Pharm. Sci. 95 (2006) 701–713.
[19] I. Flachsbart, Naturwissenschaften 44 (1957) 348.
[20] A. Levi, Atti R. Ist. Veneto 73 (1913) 185–194.
[21] J. Timmermans, F. Burriel, Chim. Ind. (1931) 196–197.
[22] J.J. Moura Ramos, N.T. Correia, H.P. Diogo, Phys. Chem. Chem. Phys. 6 (2004) 793–798.
[23] A.G. Lesnik, V.I. Danilov, Zh. Eksp. Teor. Fiz. 19 (1949) 912–915.
[24] R.B. Hammond, M.J. Jones, K.J. Roberts, H. Kutzke, H. Klapper, Z. Kristallogr. 217 (2002) 484–491.
[25] H.A.J. Oonk, J.A. Bouwstra, P.J. Van Ekeren, Calphad 10 (1986) 137–161.
[26] H.A.J. Oonk, M.T. Calvet, Equilibrium Between Phases of Matter, 1st ed., Springer, Dordrecht, 2008.
[27] H.A.J. Oonk, P.J. Eisinga, N. Brouwer, Calphad 10 (1986) 1–36.